ASSESSMENT OF SEISMIC VULNERABILITY INDEX OF GAS NETWORK AREA IN DHAKA CITY USING MICROTREMOR MEASUREMENTS

M.A. Ansary(1), A.L. Helaly(2), M. Hassan(3), M.A. Kabir(4), A. Khair(5), M.M.R. Bhuiya(6), S. Saha(7) S.A. Helaly(8)

(1) *Professor, Department of Civil Engineering, BUET, e-mail address: ansaryma66@gmail.com*
(2) *Project Director, Urban Resilience Project: RAJUK Part, e-mail address: helalyrajuk@yahoo.com*
(3) *Senior Procurement Specialist, Urban Resilience Project: RAJUK Part, e-mail address: mahboobhassan@yahoo.com*
(4) *Manager, Titas Gas and Distribution Co. Ltd., Dhaka, Bangladesh, e-mail address: kabir.engr@gmail.com*
(5) *Assistant Engineer (Civil and Geotechnical), Urban Resilience Project: RAJUK Part, e-mail address: akhairce08@gmail.com*
(6) *Assistant GIS Specialist, Urban Resilience Project: RAJUK Part, e-mail address: musfiq.sifat@yahoo.com*
(7) *GIS Expert, Jhilmil Residential Project, RAJUK, e-mail address: saha.shovon2k12@gmail.com*
(8) *Tactical Officer, Urban Resilience Project: RAJUK Part, e-mail address: rn_jfd@live.com*

Abstract

Among empirical methods, a reflexive method increasing in popularity for site response analysis is the Microtremor HVSR (H/V spectral ratio method), also commonly referred to as the Nakamura's method. The aim of this study is achieved by utilizing H/V spectral ratio method for assessment of seismic vulnerability index (K_g) of gas network area within Dhaka city. Microtremor data has been collected and analyzed in order to determine predominant frequency and amplification factor according to the guideline of SESAME. Finally, seismic vulnerability index (K_g) of site soil using Nakamura's technique has been calculated from predominant frequency and amplification factor parameter for the purpose of this research.

Fifty eight locations in and around gas network area of Dhaka city have been selected for microtremor observation. The predominant frequencies of the study area are relatively uniform, ranging from 0.36 to 1.5 Hz. The main reason for such a small range of results arises from the small differences in the near surface geological conditions of the study area. The frequencies of the study area have been grouped ranges of $0.36\text{Hz} \leq f_0 \leq 0.50\text{Hz}$, $0.51\text{Hz} \leq f_0 \leq 1.0\text{Hz}$ and $1.0\text{Hz} < f_0 \leq 1.5\text{Hz}$. It has been observed a consistent peak in a frequency range $0.36\text{Hz} \leq f_0 \leq 0.50\text{Hz}$ covered the most part of the study area. The observed frequencies can be related to the total thickness of soft sediments, deposited on the hard strata built of Madhupur tract. The low frequencies are obtained to soft soil sites in maximum measurements and the high frequencies are obtained to stiff soil sites in a few measurements. The amplification factor (A_0) or peak of H/V spectral ratio is in investigation sites ranging from 2.05 to 12.1. In the majority of the study area, the H/V spectral ratio peak amplitudes are between 2 and 6. Low values are measured for stiff soil sites and high values for soft soil sites. Variation in amplification factor and frequencies in study area have been graphically represented in ArcGIS produced maps to spatially identify the locations with higher frequencies and amplification factor.

The seismic Vulnerability Index (K_g) for 46 sites varies between 4.41 and 186.14. The low seismic vulnerability index indicates that the areas are very stiff as well as thick sediment deposit. Seismic vulnerability index (K_g) in the study area has been found that the high values are scattered in the soft alluvial deposits area having a high seismic vulnerability indication. Based on the basement ground acceleration, a_b = 0.2 g and the engineering bedrock shear wave velocity, v_b = 800 m/s, about 17.4% of the study area will face very high damage during earthquake. On the other hand, while a_b = 0.2 g and v_b = 500 m/s, about 28.3% of the study area will face very high damage during earthquake.

Keywords: H/V Spectral Ratio, Seismic Vulnerability Index, Amplification Factor, Frequency, Nakamura Technique

1. Introduction

Bangladesh is a small country situated in South Asia and bordered by India, Bhutan, and Myanmar. Its geography makes it unlike any other place on Earth. The Himalayas, the world's largest mountain range are to the north of Bangladesh. The Brahmaputra, Ganges and Meghna flow from the Himalayas and other nearby mountain ranges and amalgamate in Bangladesh. These rivers deposit huge amounts of mud and sand. Additionally, Bangladesh is one of the most tectonically active regions in the world. It sits where three tectonic plates meet: the Indian Plate, the Eurasian Plate, and the Burmese Plate. As the Indian Plate moves gradually northeast, it is slowly colliding with the Eurasian Plate, causing the Himalayas to rise. Active faults are found along this boundary, particularly the 300km-long Dauki fault that borders northern Bangladesh. Bangladesh has a long history of earthquakes. Since the last significant earthquake, Bangladesh has changed quite significantly. The greater Dhaka area has a population of over 15 million. A study of CDMP in 2011 predicted over 120,000 casualties in Dhaka due to a 7.5M earthquake [1]. There is high possibility that a huge earthquake will occur around the Himalayan region based on the difference between energy accumulation in this region and historical earthquake occurrence [2].

Although it is not possible to prevent earthquake, it is however, possible to mitigate the impacts of this disaster. Bangladesh is a country characterized by a moderate seismicity with almost no resources available for large scale seismic hazard studies. The objective of this study is to evaluate the seismic vulnerability index (K_g) using H/V spectral ratio of microtremor in terms of predominant frequency and corresponding amplification within the gas network area of Dhaka city.

2. Study Area and Site Selection

The gas is supplied through pipe of different diameter under the ground soil to gas network area of Dhaka City by Titas Gas Transmission & Distribution Company Limited. The gas network of Dhaka city consists of

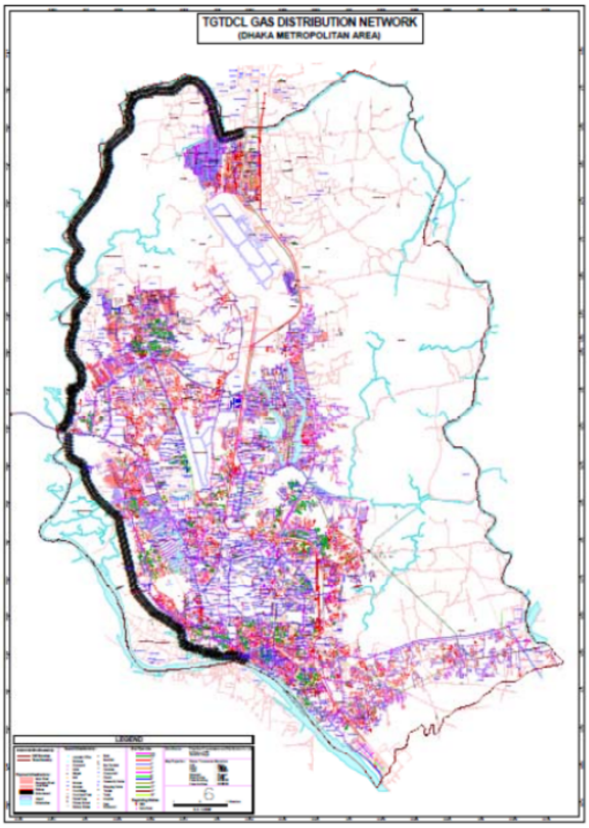

Figure. 1- Gas pipe line network of Dhaka City (Source: Titas Gas Transmission & Distribution Co. Ltd. SOB Map, 2000)

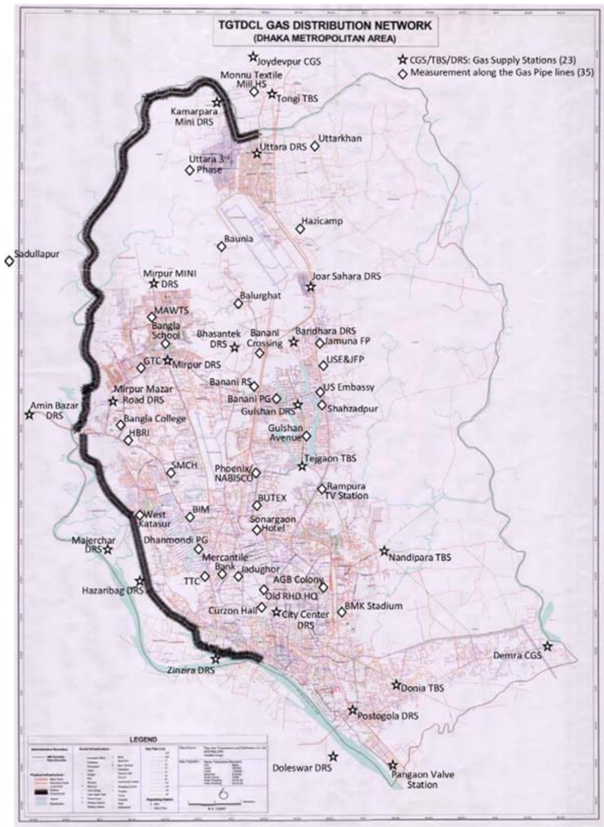

Figure. 2- Fifty-eight selected locations for microtremor observation in and around the gas network area of Dhaka city

the length of 16 inch, 14 inch, 12 inch, 10 inch, 8 inch, 6 inch, 4 inch, 3 inch and ≤ 2 inch diameter pipe is found to be 248.09 km, 173.16 km, 453.04 km, 188.01 km, 473.44 km, 371.72 km, 826.76 km, 810.64 km and 9382.01 km respectively laying beneath the ground soil about 1 m to 3 m (Figure 1). There are total 23 gas supply District Regulatory Station (DRS), Town Border Station (TBS) and City Gate Station (CGS) in the gas network of Dhaka city. To assess seismic vulnerability index (K_g) of gas network area in Dhaka city, fifty-eight locations have been selected to obtain microtremor observation (Figure 2). These microtremor observation sites are situated at latitude from 23˚40´ N to 23˚55´ N and longitude from 90˚18´ E to 90˚27´ E.

2.1 Geological Conditions of Study Area

The geology of various locations of Bangladesh is shown in Figure 3. More than 80% of Bangladesh is underlain by quaternary sediments consisting deltaic and alluvial deposits of the Ganges, Brahmaputra and

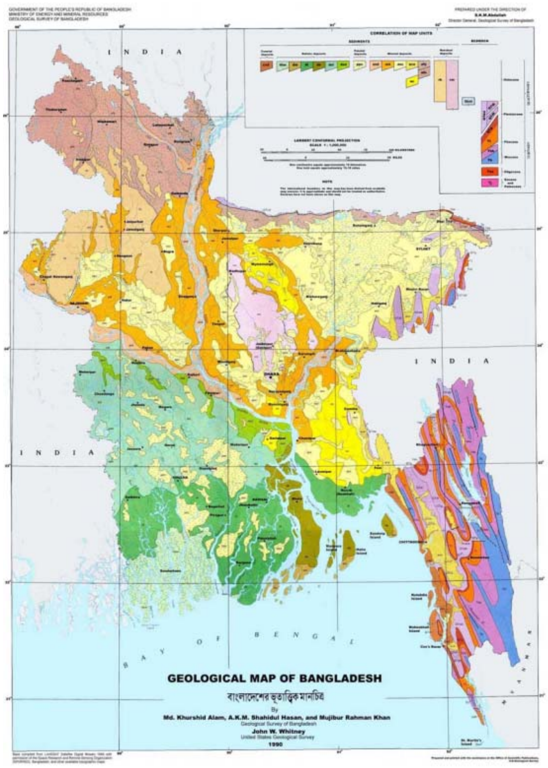

Figure. 3- Geology Map of Bangladesh. (Source: Geological Survey of Bangladesh), [3]

Meghna rivers and their tributaries. The sediments of Bangladesh Geology have been classified into five major groups, which are Coastal deposits, Deltaic deposits, Paludal deposits, Alluvial deposits and Residual deposits. These five major groups are sub-divided into sixteen different geological units. Dhaka is located between the Megna and Brahmaputra Flood Plains. The soil deposits mainly consist of the Alluvial Silt and Clay; Madhupur Clay Residuum and Marsh Clay and Peat of soil. The geology of our study area is located in three major groups, which are paludal deposits, Residual deposits and Alluvial deposits. The geological units are ppc (Marshy clay and peat), asd (Alluvial sand), asl (Alluvial silt), asc (Alluvial silt and clay) and rm (Modhupur clay residium).

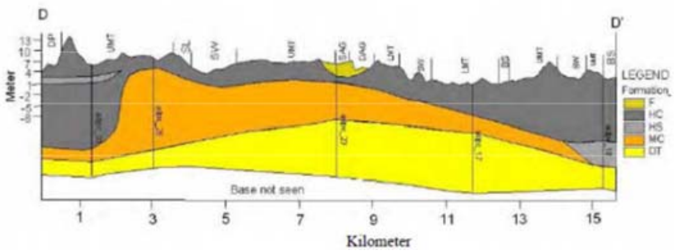

(Note: F-Fill, HC-Holocene Clay, HS-Holocene Sand, MC-Madhupur Clay and DT-Dupi Tila)

Figure 4- Schematic geological cross section of Dhaka (after CDMP, 2011)

3. Methodology

The use of microtremor, an idea pioneered by Kanai et al. (1954) turns into one of the most appealing approaches in the site effects studies, due to its relatively low economic cost, and the possibility of recordings without strict spatial or time restrictions [4]. The H/V spectral ratio technique of microtremors has gained popularity in the early nineties, after the publication of several papers claiming the ability of this technique to estimate the site response of soft sedimentary deposits satisfactorily. This method is rather attractive in developing countries characterized by a moderate seismicity, where only very limited resources are available for seismic hazard studies. The H/V spectral ratio determined from microtremors has shown a clear peak that is well correlated with the fundamental resonance frequency at "soft" soil sites [5-9]. By using the fundamental frequency and amplification factor of microtremor measurement, the value of vulnerability index (K_g) has been calculated. The ground vulnerability index (K_g) values in the liquefied areas are higher than those in the neighboring areas without liquefaction at 42 points in central Taiwan [10].

3.1 Earthquake and Microtremor Spectral Ratio

Worldwide, microtremor studies have shown that the peak amplitude of the microtremor H/V ratio tends to underestimate the peak amplitude of earthquake spectral ratios with respect to a reference (bedrock) site [11]. Numerical analysis suggests that microtremor site response can only be generated when the impedance contrast is greater than 3.5, thus the good correlation at "soft" soil sites [12]. Only a few studies claim rough agreement between the peak amplitude of the microtremor H/V ratio and earthquake site-to-reference spectral ratios [6,13,14]. In general, the site response shown by the earthquake site-to-reference spectral ratio method is regarded as the best approximation for engineering use, whereas H/V spectral ratios from earthquakes and/or microtremors are regarded as providing the fundamental peak and lower bound estimate of amplification for a soil site.

3.2 Microtremor H/V Technique

Techniques for analyzing microtremors are generally divided into two main categories: non-reference site (H/V) and reference site (H_s/H_r) techniques. A technique using horizontal to vertical spectral ratios (H/V) of the microtremors has been widely used to estimate the site effects [15-17]. Several recent applications of this technique have proved to be effective in estimating fundamental periods as well as relatively amplification factors. Two approaches for determining the site effect are the standard spectral ratio (S_T) and the H/V spectral ratio methods as shown in Figure 6 [17,18].

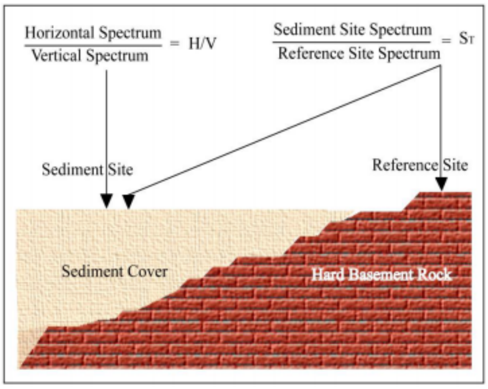

Figure. 6- Assumptions of microtremor method to derive transfer function for sedimentary basins using H/V and standard spectral ratios

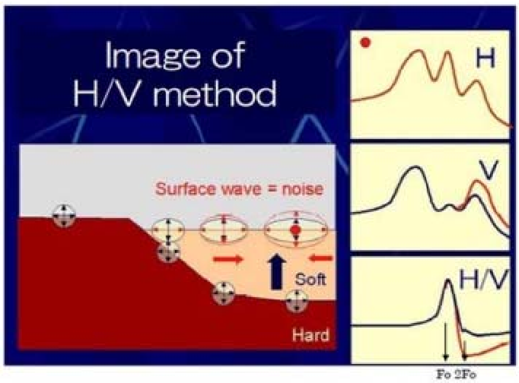

Figure. 7- Cartoon of the HVSR method, where Rayleigh wave ellipticity of the basement and ground surface is shown in the left panel. The Fourier transform of the horizontal (top) and vertical (center) component, and the resulting HVSR (bottom) are shown on the right [19].

The method use for data analysis is the Horizontal to Vertical Spectral Ratio (HVSR). The HVSR approach is applied to ambient noise and generates a Fourier spectral ratio of amplitude versus frequency. The HVSR method divides the horizontal component of noise to the vertical component to remove source effects as shown in Figure. 7. The spectral ratio is calculated by taking the Fourier transform of the ambient noise recordings. This resulting function shows how the amplitude of motion is distributed with respect to frequency. A narrow spectral peak at a particular frequency (range) implies that a large component of the energy of motion falls within that frequency range.

The HVSR approach on ambient noise recordings to clarify if this method reflected characteristics of the site as opposed to the source [20]. Their study concluded the HVSR approach was able to clearly show the HVSR peak of a sedimentary site independent of source effects.

3.3 Damage Assessment

Soil conditions are often variable even inside of a relatively small area as a town. Therefore, it is necessary to find a low-cost method to obtain a detailed dynamic characterization of soil. Microtremor is the most convenient, reliable and low-cost technique to assess the damage of any site and building. Here the Nakamura's Seismic Vulnerability Index; (K_g) method for damage assessment of any building and site has been discussed briefly.

3.3.1 Nakamura's Seismic Vulnerability Index (K_g)

Earthquake damage of structural members occurs at the time of exceeding the limit of the strain caused by deformation, and it causes the collapse if the stability of the structure lacked. Nakamura (1997) proposed use of a vulnerability index, K_g, to represent the degree to which a site or area might experience destructive ground motions, or high shear strains, during earthquakes. High shear strains (>10-6) can lead to soil liquefaction, landslide, and settlement. Nakamura (1997) investigated two areas in Japan, one largely occupied by railway lines and the other occupied by rigid-frame viaducts. Microtremor measurements were taken along railway sections that were damaged in an earthquake. These railway sections were repaired but damaged again by another earthquake. Results corresponding to K_g values along the railway line indicate that damage occurred where K_g values were relatively large [21]. Similar results were also observed in another area, where large K_g values corresponded to the amount of damage to viaducts.

Seismic vulnerability index, K_g is derived from resonant frequencies and amplification factor as determined from the H/V Ratios. For calculating K_g, shear strain of the ground is considered. Figure 8 simply shows the shear deformation of surface ground.

$$\gamma = A_g \frac{d}{h} \qquad (1)$$

Where, A is amplification factor of surface layer, h is thickness of surface layer and d is seismic displacement of the basement. Putting S-wave velocities of basement ground and surface ground as V_b and V_s respectively, proper predominant frequency F_g of surface ground is approximately expressed as,

$F_g = \dfrac{V_b}{4A_g h}$, Acceleration α_b in the basement can be written as, $\alpha_b = (2\pi F_g)^2 d$

and shear strain γ is expressed as follows,

$$\gamma = cK_g\alpha_b \qquad (2), \quad \text{Where, } c = \frac{1}{\pi^2 V_b} \text{ and } K_g = \frac{A_g^{\,2}}{F_g}$$

c is expected to be almost constant for various sites.

Figure 9 indicates K_g-values obtained in San Francisco Bay Area after the 1989 Loma-Prieta Earthquake. For Marina district the result along a line from sea coast to hillside is shown. It shows K_g at the sites where grounds deform much are bigger than 20 and K_g at the sites with no damage are very small. The result shows the similarity between actual damage and theoretical damage assessment using K_g value.

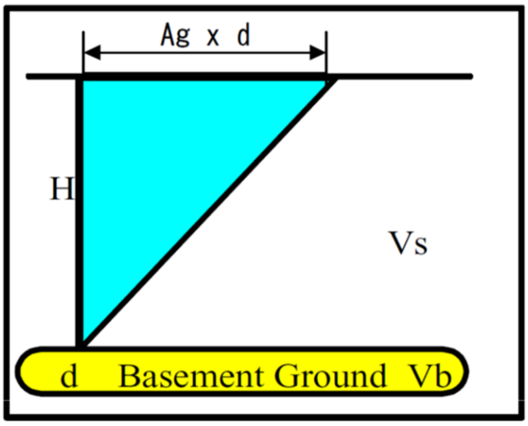

Figure. 8- Surface ground deformation.

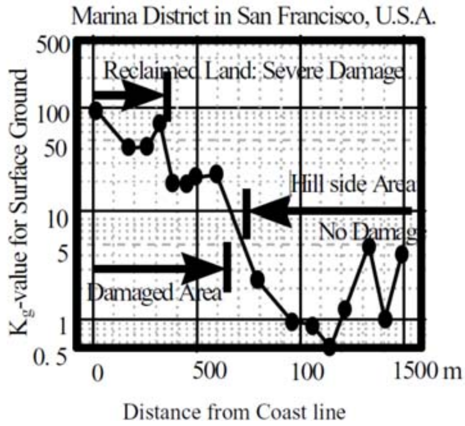

Figure. 9- K values calculated for Loma Prieta Earthquake

4. Data Collection

Microtremors are ambient vibrations of the ground caused by natural or artificial disturbances such as wind, sea waves, traffic, human activities and industrial machinery. In this study, Microtremor measurements have been performed in Dhaka city during the period January, 2015 to April, 2017. The measurements have been carried out often Friday and Saturday, the distance between sites is approximately two kilometers. Microtremor measurements have been taken at District Regulating Station (DRS), Town Bordering Station (TBS), City Gate Station (CGS) and along gas pipe lines of gas network area. Site selection and Microtremor measurements have been executed according to guideline of SESAME [22].

4.1 Guidelines of Field Data Acquisition

The information of the guidelines and criteria for the implementation of the H/V spectral ratio technique on ambient noise vibrations measurements, processing and interpretation, is currently available at the following website address:http://sesame-fpsiobs.ujf-grenoble.fr/papers/HVUserGuidelines.pdf. The reliability of the H/V technique using ambient vibrations has been investigated by SESAME European project (Site Effects assessment using Ambient Excitations). The seismological community agrees that the H/V technique gives valuable results if applied “with care” or “appropriately” [23] H/V measurements require both reliability of the results and rapidity of data collection. Therefore, avoiding the possible influence of recording parameters, asphalt, grass, cement and concrete interfaces, that of nearby buildings, that of weather conditions and stability of the results over time are very important for data quality and reliability [22].

Old RHD HQ — Teachers Training College

Figure 10- Microtremor data recording in and around Dhaka city.

4.2 Data Recording

The total recording duration should be increased; in order to remove some transients occurred during the recording, from the signal for processing for “good quality” signal windows (SESAME, WP12, 2004). In this study microtremor data has been recorded for 30 minute according to SESAME recommendation.

Velocity-time history field microtremor data has been recorded in GeoDAS software with suitable five number of observation channels/sensors, 15m observation length, 200 Hz observation frequency, specific low or high pass filter code, amplification ratio, observation latitude and longitude, observation time and observation channel mode. Figure 11 shows a typical time history field data recording of

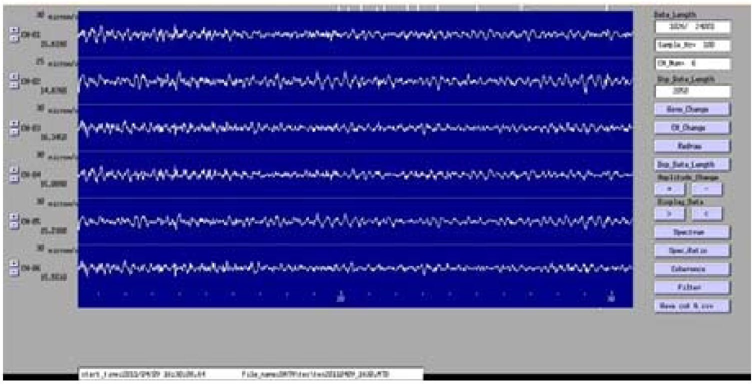

Figure. 11- Time history of Microtremor observation at MT16-Mirpur 10 DRS

MT1-Mirpur 10 DRS at 11:30 PM on 6 February, 2016. The content of all input data are 2 CR-6plus velocity type sensors, 360000 observation points, 200Hz sampling frequency, 0.05 Hz Low-pass filter, 20db amplification ratio, Latitude-23°48'25.5"N and Longitude-90°22'08.1"E.

5. Data Analysis and Processing

Several methods have been proposed for spectral calculation of ground motions including microtremor. Fourier spectrum is the most convenient one that is used widely. Some investigations showed that different methods give similar results. However, some researchers declare that a suitable spectral method gives more reliable results [24]. That’s why minimum twenty-five windows have been selected from time history to compute amplitude spectrum of all three components, amplitude spectral ratios and the mean spectral ratio. Standard deviation of mean has also been calculated to show the deviation of mean value from twenty-five spectral ratios.

5.1 H/V Spectral Ratio Methodology

After the collection of data using the acquisition software with recommendations, precautions and any other requirements from SESAME guidelines and from other experts, the data has been compiled for each site in order to analyze them using DPLOT software. DPLOT is a windows program that lets engineers create presentation quality graphs from a wide variety of data sources. However, SESAME has developed a software for data analysis applying the H/V technique. The name of the software is J-SESAME to be used as a standard procedure in processing the microtremor data using H/V technique.

5.1.1 H/V Spectral Ratio Curve Generation

Time history data is not suitable to estimate the dynamic properties (predominant frequency and amplification ratio). So, transformation of time domain data to frequency domain data is required with Fourier Transformation. Only the Fourier Spectrum along three subsequent directions is not appropriate to estimate the predominant frequency and amplification. So, Horizontal to Vertical spectral ratio (H/V) is required to determine the dynamic properties of soil. After smoothing the corresponding curves, the output result, as shown in Figure 12, shows the H/V spectral ratio is the black continuous curve and it lies between the upper and lower standard deviation curves (dashed curve). From this graph, it has been observed that the range of frequency where in the H/V amplification is maximum. This range of frequency contains the predominant frequency (f_0) of the site. The peak value in the H/V solid curve represents the average value for the wave amplification factor (A_0) at that site. Seismic vulnerability index (K_g) has been determined using the predominant frequency (f_0) and amplification factor (A_0) of this site as, $K_g = \frac{A_0^{\,2}}{f_0}$.

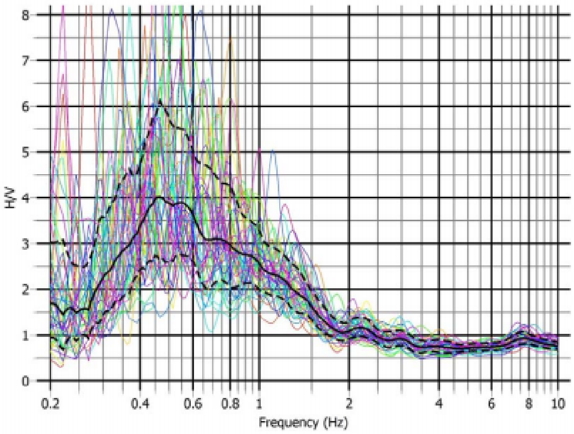

Figure 12- H/V spectral ratio curve of MT16- Mirpur 10 DRS site

5.1.2 Criteria of the H/V Spectral Ratio Analysis

The SESAME guidelines have three conditions for H/V spectral ratio curve reliability and five out of six criteria for identification of a peak frequency, f_0, as a clear peak. These criteria are depicted in Figure 13.

Criteria for a reliable H/V curve

i) $f_0 > 10 / l_w$

and

ii) $n_c (f_0) > 200$

and

iii) $\sigma_A(f) < 2$ for $0.5f_0 < f < 2f_0$ if $f0 > 0.5Hz$

or $\sigma_A(f) < 3$ for $0.5f_0 < f < 2f_0$ if $f0 < 0.5Hz$

Criteria for a clear H/V peak

(at least 5 out of 6 criteria fulfilled)

i) $\exists f^- \in [f_0/4, f_0] \mid A_{H/V}(f^-) < A_0/2$

ii) $\exists f^+ \in [f_0, 4f_0] \mid A_{H/V}(f^+) < A_0/2$

iii) $A_0 > 2$

iv) $f_{peak}[A_{H/V}(f) \pm \sigma_A(f)] = f_0 \pm 5\%$

v) $\sigma_f < \varepsilon(f_0)$

vi) $\sigma_A(f_0) < \theta(f_0)$

- l_w = window length
- n_w = number of windows selected for the average H/V curve
- $n_c = l_w \cdot n_w \cdot f_0$ = number of significant cycles
- f = current frequency
- f_{sensor} = sensor cut-off frequency
- f_0 = H/V peak frequency
- σ_f = standard deviation of H/V peak frequency ($f_0 \pm \sigma_f$)
- $\varepsilon(f_0)$ = threshold value for the stability condition $\sigma_f < \varepsilon(f_0)$
- A_0 = H/V peak amplitude at frequency f_0
- $A_{H/V}(f)$ = H/V curve amplitude at frequency f
- f^- = frequency between $f_0/4$ and f_0 for which $A_{H/V}(f^-) < A_0/2$
- f^+ = frequency between f_0 and $4f_0$ for which $A_{H/V}(f^+) < A_0/2$
- $\sigma_A(f)$ = "standard deviation" of $A_{H/V}(f)$, $\sigma_A(f)$ is the factor by which the mean $A_{H/V}(f)$ curve should be multiplied or divided
- $\sigma_{logH/V}(f)$ = standard deviation of the $\log A_{H/V}(f)$ curve, $\sigma_{logH/V}(f)$ is an absolute value which should be added to or subtracted from the mean $\log A_{H/V}(f)$ curve
- $\theta(f_0)$ = threshold value for the stability condition $\sigma_A(f) < \theta(f_0)$
- $V_{s,av}$ = average S-wave velocity of the total deposits
- $V_{s,surf}$ = S-wave velocity of the surface layer
- h = depth to bedrock
- h_{min} = lower-bound estimate of h

Threshold Values for σ_f and $\sigma_A(f_0)$

Frequency range [Hz]	< 0.2	0.2 – 0.5	0.5 – 1.0	1.0 – 2.0	> 2.0
$\varepsilon(f_0)$ [Hz]	0.25 f_0	0.20 f_0	0.15 f_0	0.10 f_0	0.05 f_0
$\theta(f_0)$ for $\sigma_A(f_0)$	3.0	2.5	2.0	1.78	1.58
$\log\theta(f_0)$ for $\sigma_{logH/V}(f_0)$	0.48	0.40	0.30	0.25	0.20

Figure 13- H/V Spectral Ratio testing criteria set forth by SESAME. Clockwise from top left panel: Criteria for reliable curve, variable list and description, threshold values for standard deviation of frequency and amplitude, and criteria for clear peak. Image is from SESAME, WP12.

6. Results and Discussions

The measurements consisted of 58 microtremor measurements. Each measurement consists of thirty minutes recording. Following the SESAME recommendations, frequency peaks with amplitude greater than 2 has been measured [22]. Total 46 out of 58 microtremor measurements have been considered to determine the site fundamental period and amplification factor. These 46 curves produced reliable curves.

Figure 14 shows the distribution of f_0 where the distribution of predominant frequencies is relatively uniform, ranging from 0.36 to 1.5 Hz. Obviously, the red color delineates high values of fundamental frequency located in the central part and the edge of northing, southing and easting part of the study area reaching 1.5 Hz while the blue color represents the low values of fundamental frequency in the round of central part of the study area reaching 0.36 Hz. Figure 15 represents the amplification factor (A_0) or peak of H/V spectral ratio in investigation sites ranging from 2.05 to 12.1. The red color reveals the high values of amplification factor reaching 12.1 while the blue color illustrates the low values. High amplification factor ($A_0 > 4$) has been found in the northern part of the study area.

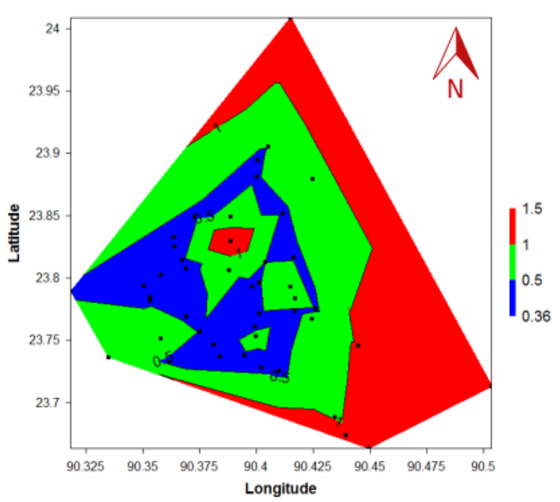

Figure. 14- Distribution of the fundamental frequency (f_0) in the study area

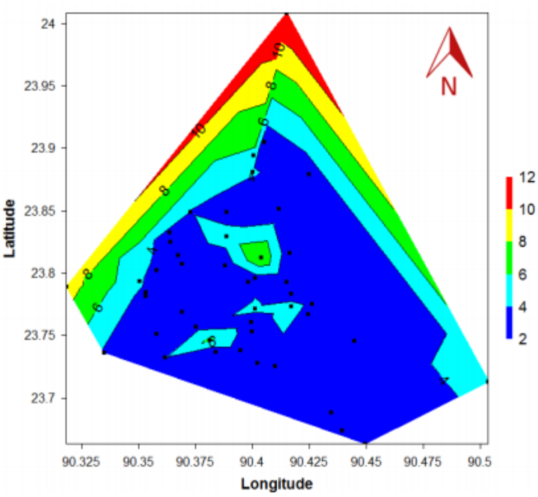

Figure. 15- Distribution of the Amplification factor (A0) in the study area.

6.1 Calculation of Seismic Vulnerability Index, K_g

Nakamura (1997) introduced a vulnerability index parameter (K_g), which combined amplification factor (A_0) and predominant frequency (f_0) to identify areas where greater seismic hazards and damage may be expected using H/V spectral ratio technique. Some studies showed a good correlation between seismic vulnerability index (K_g) and the distribution of earthquake disaster damage [10,25]. Thus, K_g value reflects local site effect and can be considered as an indicator which might be useful in selecting weak point of ground. Therefore, this index has been used for the detection of gas network areas of Dhaka City that are weak zone at the time of occurrence of earthquakes. As sample, calculated K_g values for 10 locations of the study area are shown in Table 1.

Table 1- Seismic vulnerability index K_g value of few points within the study area

Sl. No	ID	Location	Latitude	Longitude	Predominant Frequency, f_0 (Hz)	H/V Ratio, A_0	Vulnerability Index, K_g	*Remarks
1	MT1	Mirpur 10 DRS	23°48'25.5"N	90°22'08.1"E	0.46	4.00	34.78	Very High
2	MT2	Tongi TBS	23°54'17.47"N	90°24'18.71"E	0.51	2.81	15.48	High

Sl. No	ID	Location	Latitude	Longitude	Predominant Frequency, f_0 (Hz)	H/V Ratio, A_0	Vulnerability Index, K_g	*Remarks
3	MT3	Kamarpara DRS	23°52'50.8"N	90°24'00.9"E	0.48	4.20	36.75	Very High
4	MT4	Uttara DRS	23°52'26.8"N	90°23'58.3"E	-	-	-	-
5	MT5	Uttarkhan	23°52'45.0"N	90°25'29.3"E	0.75	2.72	9.86	Moderate
6	MT6	Uttara 3rd Phase	23°50'55.3"N	90°22'22.0"E	0.41	3.88	36.72	Very High
7	MT7	Hazi Camp	23°51'04.1"N	90°24'41.3"E	0.44	2.38	12.87	High
8	MT8	Baunia	23°50'57.0"N	90°23'18.7"E	0.59	2.91	14.35	High
9	MT9	Joarsahara DRS	23°49'48.9"N	90°25'08.0"E	-	-	-	-
10	MT10	Balurghat	23°49'46.4"N	90°23'19.1"E	1.48	4.85	15.89	High

The common base rock under the Dhaka region is situated at a depth of approximately 10 km [26]. The peak ground acceleration of Dhaka is 0.2 g [27]. Assuming a_b = 0.2 g and engineering bedrock shear wave velocity, v_b = 800 m/s, for $\gamma > 1000\times10^{-6}$ then the K_g value > 4.0; and for $\gamma > 10{,}000\times10^{-6}$ the K_g value > 40.0. Based on the above criteria, for the value of K_g > 4.0 has been found to spread throughout the study area and for the value of K_g > 40 has been found only at several sites of the study area. The seismic vulnerability index value has been classified into four major types of damage. These are Low (0 to ≤ 4.0), Moderate (< 4.0 to ≤ 20), High (< 20 to ≤ 40) and Very High (>40). Thus, the higher K_g values (K_g > 40) in the site of gas network area has been considered as weak zones which may cause very high damage to infrastructure located in those area during an earthquake.

Figure 16 illustrate the distribution of vulnerability index (K_g) having values ranging from 4.41 to 186.14. Seismic vulnerability index (K_g) in the study area has found that the high values are scattered in the alluvial deposits area having a high seismic vulnerability indication. Figure 17, shows about 17.4% of research area of gas network are most vulnerable causing very high damage during earthquake. There are also 0% low, 58.7% moderate and 23.9% high damage area of 46 investigated sites.

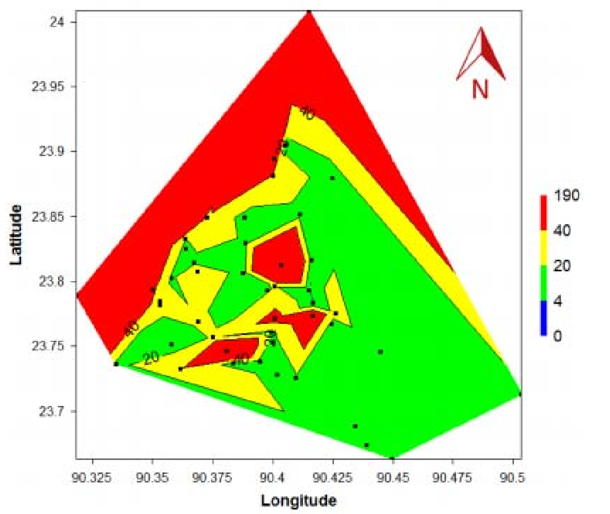

Figure 16- Contour map of the K_g value based on engineering bedrock shear wave velocity 800 m/s in the study areas. The higher K_g values appear in the northern area.

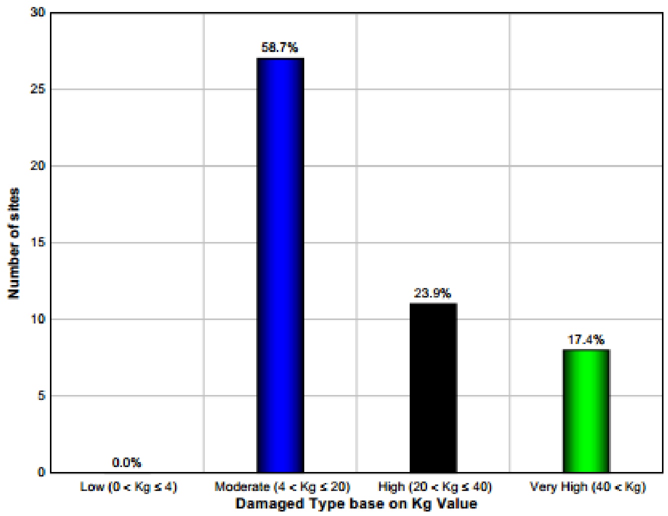

Figure 17- Distribution of damage area based on vulnerability index (Kg)

7. Conclusions

Microtremor measurements have been performed in Dhaka city during the period January, 2015 to April, 2017. Microtremor data of 58 sites have been recorded using broad band sensor type of three component seismograph "Central Recording System (CR-6plus)" produced by GeoSIG Ltd. The CR-6plus seismograph consists of GeoDAS software, 15 channel, 24 bit acquisition box system with built-in computer with all its auxiliary peripherals. The sampling rate was set to 200 Hz and the duration of recording 30 minutes. These data are acquired according to guidelines of SESAME, WP12-Deliverable D23.12, 2004.

Microtremor measurements of 46 sites have produced reliable curves and peaks of H/V spectral ratio to determine the site fundamental period and amplification factor. It is not possible to determine the fundamental frequency and amplification factor for 12 sites due to unreliable curve and flat curve. The predominant frequencies of the study area are relatively uniform, ranging from 0.36 to 1.5 Hz. The main reason for such a small range of results arises from the small differences in the near-surface geological conditions of the study area. The frequencies of the study area have been grouped ranges of $0.36Hz \leq f_0 \leq 0.50Hz$, $0.51Hz \leq f_0 \leq 1.0Hz$ and $1.0Hz < f_0 \leq 1.5Hz$. It has been observed a consistent peak in a frequency range $0.36Hz \leq f_0 \leq 0.50Hz$ covered the most part of the study area.

Seismic vulnerability index (K_g) is calculated from the predominant frequency and amplification factor for 46 sites. Seismic vulnerability index (K_g) is an index indicating the level of vulnerability of a layer of soil to deform at the time of occurrence of earthquakes. The range of seismic vulnerability index (K_g) value is determined assuming the basement ground acceleration, a_b = 0.2 g and engineering bedrock shear wave velocity, v_b = 800 m/s. It has been observed that the K_g value > 4.0 for $\gamma > 1000 \times 10^{-6}$ and the Kg value > 40.0 for $\gamma > 10{,}000 \times 10^{-6}$. The value of K_g > 4.0 has been found to spread throughout the study area and the value of K_g > 40 has been found only at several points of the study area. The seismic vulnerability index (K_g) value has been classified into four major types of damage. These are Low (0 to ≤ 4.0), Moderate (< 4.0 to ≤ 20), High (< 20 to ≤ 40) and Very High (>40). Thus, the higher Kg values (K_g > 40) in the site of gas network area has been considered as weak zones which may damage during the earthquake. The high values of vulnerability index K_g > 40 in the northern part of the study area may cause very high damage while the low values of the vulnerability index being $4 < K_g \leq 20$ may cause moderate damage. 17.4% of research area of gas network is most vulnerable causing very high damage during earthquake. There are also 0% low, 58.7% moderate and 23.9% high damage area of 46 investigated sites.

8. Reference

[1] CDMP (2011). Comprehensive Disaster Management Program (CDMP), Bangladesh, Seismic hazard and vulnerability mapping of Dhaka, Chittagong, and Sylhet city corporation areas, 2011.

[2] Bilham, R., Gaur, V. K. and Molnar, P. (2001). Himalayan Seismic Hazard, SCIENCE, 293.

[3] Alam. M.K., Hasan, A.K.M.S., Khan, M.R., and Whitney, J.W. (1990). Geological map of Bangladesh. Geological Survey of Bangladesh, Dhaka.

[4] Rodriguez, V. S. H. and Midorikawa, S. (2002). Applicability of the H/V Spectral Ratio of Microtremors in Assessing Site Effects on Seismic Motion, Earthquake Engineering and Structural Dynamics, 31, PP. 261 -279.

[5] Bard, P. Y. (2004). Effects of surface geology on ground motion: Recent results and remaining issues, Proceedings of the 10th European Conference on Earthquake Engineering, Vienna, Austria, August 28 - September 2, 1994, PP. 305-325.

[6] Horike, M., Zhao, B. and Kawase, H. (2001). Comparison of site response characteristics inferred from microtremors and earthquake shear waves, Bulletin of the Seismological Society of America, 91, PP. 1526-1536.

[7] Field, E. H. and Jacob, K. H. (1995). A comparison and test of various site-response estimation techniques, including three that are not reference-site dependent, Bulletin of the Seismological Society of America, 85, PP. 1127-1143.

[8] achet, C. and Bard, P. Y. (1994). Numerical and theoretical investigations on the possibilities and limitations of Nakamura's technique, Journal of the Physics of the Earth, 42, PP. 377-397.

[9] Lermo, L. and Chavez-Garcia, F. J. (1993). Site effect evaluation using spectral ratios with only one station, Bull. Seism. Soc. Am., 83, PP. 1574-1594.

[10] Huang, H. C., (2002). Characteristics of earthquake ground motions and the H/V of microtremors in the southwestern part of Taiwan: Earthquake Engineering and Structural Dynamics, 31, 1815-1829.

[11] Bard, P. Y. (1998). Microtremor measurements: A tool for site effect estimation? Proceedings of the second international symposium on the effects of surface geology on seismic motion, Yokohama, Japan, December 1998, PP. 1251 -1279.

[12] Malischewsky, P. G. and Scherbaum, F. (2004). Love's formula and H/V-ratio (ellipticity) of Rayleigh waves, Wave Motion, 40, PP. 57-67.

[13] Molnar, S. and Cassidy, J. F. (2006). A comparison of site response techniques using weak-motion earthquake and microtremors, Earthquake Spectra, 22, PP. 169-188.

[14] Mucciarelli, M., Gallipoli, M. R. and Arcieri, M. (2003). The stability of the horizontal to vertical spectral ratio of triggered noise and earthquake recordings, Bulletin of the Seismological Society of America, 93 (3), PP. 1407-1413.

[15] Nogoshi, M. and Igarashi, T. (1970). On the propagation characteristics of microtremors. J. Seism. Soc. Japan, 23, PP. 264-280 (in Japanese with English abstract).

[16] Nogoshi, M., and Igarashi, T. (1971). On the amplitude characteristics of microtremor (Part 2), Journal of the Seismological Society of Japan, 24, PP. 26-40.

[17] Nakamura, Y. (1989). A Method for Dynamic Characteristics of Sub-surface Using Microtremors on the Ground Surface, Quick Report of Railway Technical Research Institute, 30, No. 1, PP. 25-33 (in Japanese).

[18] Katz, L. J. (1976). Microtremor analysis of local geological conditions: Bulletin of the Seismological Society of America, 66, 45-60.

[19] Nakamura, Y. (2008). On the H/V spectrum. The 14th World Conference on Earthquake Engineering, 1-10.

[20] Lachet, C. and Bard, P. Y. (1994). Numerical and theoretical investigations on the possibilities and limitations of Nakamura's technique, Journal of the Physics of the Earth, 42, PP. 377-397.

[21] Nakamura, Y. (1997). Seismic Vulnerability Indices For Ground and Structures Using Microtremor, World Congress on Railway Research in Florence, Italy, November 1997.

[22] SESAME WP12, (2004). Guidelines for the implementation of the H/V spectral ratio technique on ambient vibrations. Measurements, processing and interpretation. SESAME European research project. European Commission. Research General Directorate Project No. EVG1 -CT-2000-00026 SESAME, D23.12. http://sesamefp5.obs.ujf grenoble.fr/SES_TechnicalDoc.htm.

[23] Martin G. Koller, Jean-Luc Chatelain, Bertrand Guillier, Anne-Marie Duval, Kuvvet Atakan, Corinne Lacave, Pierre-Yves Bard and the SESAME participants (2004). Practical User Guidelines and Software for the Implementation of the H/V Ratio Technique: Measuring Conditions, Processing Method and Results Interpretation, 13th World Conference on Earthquake Engineering, Vancouver, B.C., Canada, August 1 -6, 2004, Paper No. 3132

[24] Ghayamghamian, M. R. and Kawakami, H. (1997). Segmental cross-spectrum in microtremor spectral ratio analysis. 7th International Conference on Structural Safety and Reliability, Kyoto, November 1997, 24-28, PP. 1487-1494.

[25] Nakamura, Y. (2000). Clear identification of fundamental idea of Nakamura's Technique and its applications, Proc. Of the 12th World Conference on Earthquake Engineering, Auckland, New Zealand, PP. 2656-2664.

[26] Khan, A. H. (1990). Geology of Bangladesh, University Press Limited.

[27] BNBC (Draft 2017). Bangladesh National Building Code, 2017. HBRI-BSTI.

